

## Magnetic form factor of Cu in $\text{La}_2\text{CuO}_4$

T. Freltoft and G. Shirane

*Brookhaven National Laboratory, Upton, New York 11973*

S. Mitsuda

*Institute for Solid State Physics, University of Tokyo, Tokyo 106, Japan*

J. P. Remeika and A. S. Cooper

*AT&T Bell Laboratories, Murray Hill, New Jersey 07974*

(Received 21 September 1987)

The magnetic form factor for Cu in a single crystal of the antiferromagnet  $\text{La}_2\text{CuO}_4$  has been measured using neutron diffraction. The result is consistent with the calculation of Freeman and Watson for  $\text{Cu}^{2+}$  at least up to  $Q=4 \text{ \AA}^{-1}$ , although a plateau between 1 and  $3 \text{ \AA}^{-1}$  suggests a small contribution of moment at the out-of-plane oxygen sites. For larger values of  $Q$  the form factor for  $\text{La}_2\text{CuO}_4$  drops faster than for  $\text{Cu}^{2+}$ . The sample ordered antiferromagnetically at  $T_N \approx 185 \text{ K}$  with an average ordered moment  $\mu = 0.30 \mu_B$  per Cu atom.

### I. INTRODUCTION

Since the discovery<sup>1</sup> of high- $T_c$  superconductivity in  $\text{La}_{2-x}(\text{Ba,Sr})_x\text{CuO}_4$  a tremendous effort has been devoted to the study of these materials and their parent compound  $\text{La}_2\text{CuO}_4$ . The interesting question is to determine the nature of the interactions leading to the superconducting phase. Several mechanisms have been suggested<sup>2</sup> among which are the original electron-phonon coupling of the Bardeen-Cooper-Schrieffer (BCS) theory, charge or spin-density pictures, a theory where the charge carriers are holes in the oxygen ( $2p$ ) states and the pairing is mediated by strong coupling to local spin configurations on the Cu sites, and a theory where the charge carriers are topological defects in a resonating-valence-bond state. Recently it has been established<sup>3,4</sup> that  $\text{La}_2\text{CuO}_{4-\delta}$  undergoes an antiferromagnetic phase transition and the Néel temperature  $T_N$  and ordered moment  $\mu$  were found<sup>5-7</sup> to depend strongly on the oxygen deficiency  $\delta$ . For  $\delta=0$  no magnetic ordering is observed down to  $T=5 \text{ K}$  and for increasing  $\delta$ , both  $T_N$  and  $\mu$  increase up to  $T_N \approx 300 \text{ K}$  and  $\mu = 0.4 \mu_B$  per Cu atom.

In previous papers concerning the magnetic properties of  $\text{La}_2\text{CuO}_4$  it is assumed that the relevant magnetic form factor is that of  $\text{Cu}^{2+}$  as measured in the ferromagnet  $\text{K}_2\text{CuF}_4$ , but so far this has not been verified experimentally. Only Ref. 3 reports preliminary powder measurements of the form factor for four magnetic reflections. The magnetic form factor is the Fourier transform of the spin-density distribution around the magnetic atom, and hence, a determination of this may give important information related to the possibility of magnetic correlations being responsible for the superconducting properties in the doped materials. In this paper we present a neutron-diffraction study of a single crystal of  $\text{La}_2\text{CuO}_4$ . We characterize the sample in terms of crystal and magnetic structures, orthorhombic distortion, antiferromagnetic transition temperature, ordered magnetic moment, magnetization curve, and magnetic form factor. We also discuss in detail the experimental difficulties concerning extinction effects and multiple Bragg scattering.

### II. EXPERIMENTAL PROCEDURE

#### A. Sample

It is difficult to grow sizable single crystals from stoichiometric melts of  $\text{La}_2\text{CuO}_4$  because of the high peritectic melting temperature of 1640 K. The present crystals are grown using a flux growth technique and a cooling rate of  $\approx 10^\circ\text{C/h}$ . In this way platelike single crystals of  $\sim 2 \text{ mm}^3$  have been grown. It is now well established<sup>5-7</sup> that different heat treatments in a vacuum of  $\text{La}_2\text{CuO}_4$  crystals from the *same* batch will produce systems with systematically varying antiferromagnetic transition temperatures and average ordered moments. We use a piece of clean Zr foil to act as  $\text{O}_2$  getter in the evacuated  $\text{SiO}_2$  tube along with the crystals being reduced. Thus, one achieves quantitative and reproducible  $\text{O}_2$  removal for any given reaction temperature. In previous work<sup>5</sup> we found that the *as grown* crystal ordered at  $T_N \approx 50 \text{ K}$ . However, *as grown* crystals from different batches may not exhibit exactly the same oxygen deficiency due to small variations in the relative amount of the constituents or other preparation conditions. Hence, the specific properties of *as grown* crystals which depend on the oxygen content may not in general be compared directly. As has been discussed earlier,<sup>5</sup> the exact oxygen content is very difficult to estimate, and although *as grown* crystals are believed to be close to stoichiometry ( $\delta=0$ ), we have found that heat treatment of the crystals in oxygen atmosphere at  $800^\circ\text{C}$  for 16 h results in no antiferromagnetic ordering down to 4.2 K. This indicates that oxygen vacancies are already present in the *as grown* crystals since it is unlikely that an excess of oxygen ( $\delta < 0$ ) is present in the sample. This effect has also been observed for powder samples of  $\text{La}_2\text{CuO}_4$  by Johnston *et al.*<sup>6</sup>

$\text{La}_2\text{CuO}_4$  crystalizes in the  $\text{K}_2\text{CuF}_4$  tetragonal structure (space group  $I4/mmm$ ) and exhibits a tetragonal-to-orthorhombic phase transition<sup>8</sup> around  $T=500 \text{ K}$ . In the orthorhombic phase (space group  $Cmca$ ) the unit cell doubles so that if the tetragonal unit cell is  $(a, a, c)$ , the orthorhombic cell corresponds to  $(\sqrt{2}a - \epsilon, c, \sqrt{2}a + \epsilon)$ . In

this notation, the orthorhombic (200) reflection is equivalent to the tetragonal (110). Since all measurements in this paper are performed in the orthorhombic phase we use the orthorhombic notation. Recently it has been suggested that the space groups for  $\text{La}_2\text{CuO}_4$  are not the ones given above, but rather  $Pccm$  and  $Pccn$  for the tetragonal and orthorhombic phases, respectively.<sup>9</sup> However, the calculated intensities of the neutron Bragg reflections for the two sets are almost identical. Hence, we are not able to distinguish between the two models, and it has no practical influence on the interpretation of our data.

The orthorhombic distortion causes a twin structure to develop in this phase. Therefore, alternating orientations of the  $a$  and  $c$  directions occur, and hence, in a diffraction experiment both  $(hk0)$  and  $(0kl)$  reflections will be observed concurrently. [I.e., the orthorhombic distortion manifests itself by a splitting of the original tetragonal peaks in the (100) direction.] This is depicted in Fig. 1 where the scattering plane for the present experiment is shown. The splitting is exaggerated for clarity. The size of the twin domains is found from electron microscopy<sup>10</sup> to be of the order 1000 Å.

Among the  $\text{La}_2\text{CuO}_4$  samples prepared for the study of

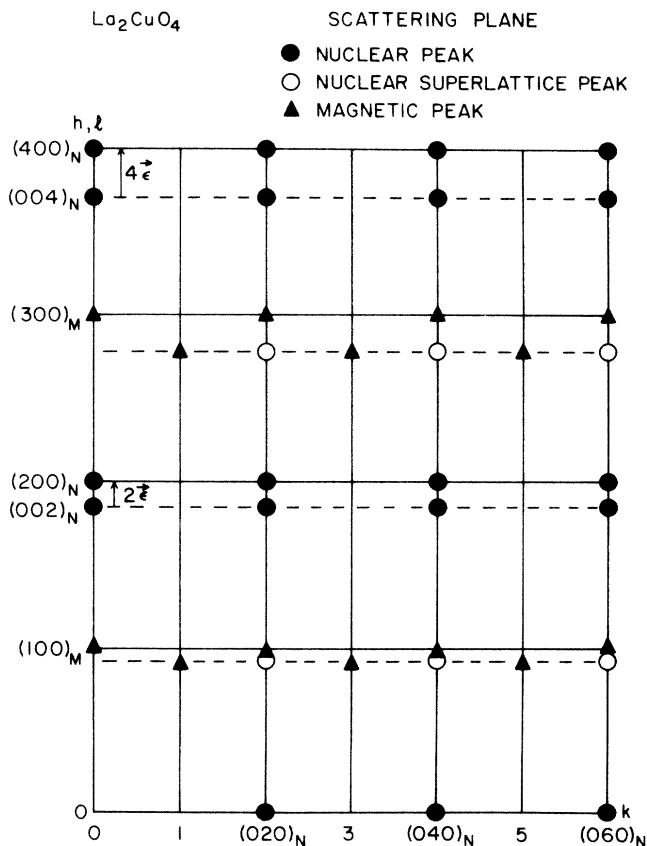


FIG. 1. Scattering plane in the antiferromagnetically ordered phase for the  $\text{La}_2\text{CuO}_4$  crystal as oriented in the present experiment. The twin-domain structure created by the orthorhombic distortion implicates that both the  $(100)$  and  $(001)$  directions are always present simultaneously.

oxygen deficiency effects we chose a crystal with Néel temperature  $T_N \approx 185$  K for the present work. This crystal is denoted  $A$ . The unit-cell dimensions are  $a=5.331$  Å,  $b=13.10$  Å, and  $c=5.412$  Å at  $T=10$  K, and hence, the orthorhombic distortion  $c/a-1$  is 1.50%. An extensive investigation of extinction effects was performed on a similar sample denoted  $B$  with  $T_N \approx 200$  K. Lattice parameters and distortion were not significantly different for the two crystals.

## B. Neutron diffraction measurements

The measurements were conducted at the Brookhaven High-Flux Beam Reactor on the triple-axis spectrometer H4M. Pyrolytic graphite (PG) (002) reflections were used as both monochromator and analyzer, and a PG filter after the sample was used to suppress higher-order contamination of the diffracted beam. Most of the data were taken with an incoming neutron energy of 13.4 meV ( $k_i=k_f=2.543$  Å<sup>-1</sup>), and to study higher momentum transfers some data were also taken at 31.0 meV ( $k_i=k_f=3.868$  Å<sup>-1</sup>). These incident energies were found to exhibit the smallest amount of multiple Bragg scattering within the energy windows provided by the PG filter. The spectrometer was operated in a  $\theta-2\theta$  mode, stepping constant values of  $\Delta\theta$  to ensure that all integrated intensities could be compared directly using the relation

$$\sum_{\theta} I(\theta, 2\theta) = A \frac{|F|_{\text{obs}}^2}{\Delta\theta \sin(2\theta_B)}, \quad (1)$$

where  $I(\theta, 2\theta)$  is the background-subtracted neutron count rate measured at the angle  $\theta$ ,  $2\theta_B$  is the angle of the Bragg peak position,  $A$  is an instrument scale factor, and  $|F|_{\text{obs}}$  is the observed structure factor. The collimation was chosen as  $20'-20'-20'-80'$  which, for  $E_i=13.4$  meV and  $\Delta 2\theta \approx 0.05^\circ$ , is tight enough to resolve the orthorhombic distortion at  $T=10$  K.

## C. Multiple Bragg scattering

One of the major experimental difficulties when working with single crystals is multiple Bragg scattering. This occurs when the crystal is so oriented in the beam that two, or more, sets of planes satisfy Bragg's law for a single incident neutron energy. One way of estimating the amount of multiple scattering at a specific point in the scattering plane is to perform an elastic energy scan where the incoming and detected neutron energies are both varied simultaneously while keeping the momentum transfer (i.e., the scattering vector  $\mathbf{Q}$ ) constant. If multiple scattering is possible for the  $\mathbf{Q}$  in question, the elastic energy scan will typically exhibit some structure in the form of double scattering peaks. Hence, it is possible for a specific position in the scattering plane to find incident neutron energies which are "clean" by choosing an incident energy far from such peaks.

The possibility of *double* Bragg scattering in a specific

point can be determined by simple inspection of the scattering plane, see Fig. 1. The condition for a double scattering process to appear at the position  $\mathbf{H}$  is that there exist reciprocal lattice vectors  $\mathbf{H}_1$  and  $\mathbf{H}_2$  such that  $\mathbf{H} = \mathbf{H}_1 - \mathbf{H}_2$ . If we initially only consider double scattering processes among nuclear reflections and only within one twin domain, it can be seen from Fig. 1, that double scattering may occur at, e.g., the (001), (003), ... positions, but not at (100), (300), etc. However, if we also consider double scattering events between different twin domains, the picture is much more complicated. In this case we may expect additional peaks at any position

$(100) \pm n\epsilon$ , where  $n$  is an integer and  $\epsilon$  is defined as the vector in the scattering plane between the (001) and (100) positions (see Fig. 1). The length of  $\epsilon$  is related to the orthorhombic distortion,  $\epsilon/c^* = c/a - 1$ . Double scattering between different twin domains is not commonly expected, but occasionally we have observed a peak at the  $(100) + \epsilon$  which was as strong as the magnetic (100) reflection itself. Since the double scattering effects are coupled to the orthorhombic distortion which is temperature dependent, the appearance of additional peaks was also found to change with temperature.

In Fig. 2 is shown elastic energy scans at a representative selection of positions close to (or at) magnetic reflections in the scattering plane. The scans were performed for incident neutron energies ranging from 13 to 15 meV, within the energy window provided by the PG filter. It may be seen from the figure that multiple Bragg scattering effects are of great importance for the present system, especially at the (001) and (003) positions. Fortunately we found that the incident neutron energy  $E_i = 13.4$  meV (broken line) provided a sufficiently clean signal for all

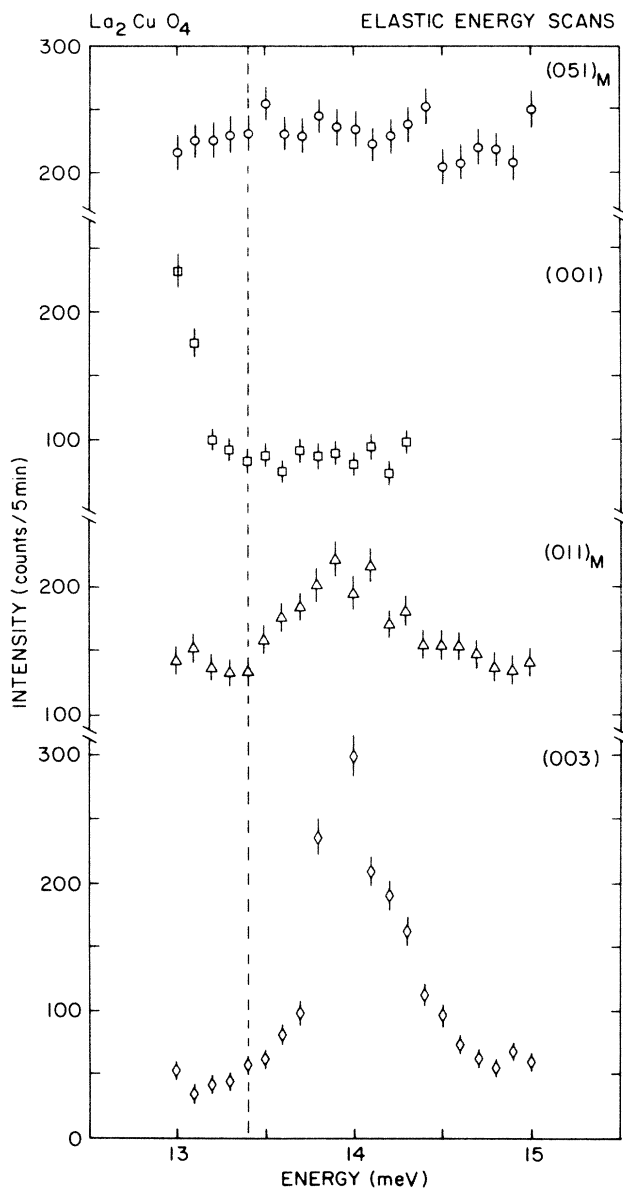


FIG. 2. Elastic energy scans at selected positions in the scattering plane. The effect of multiple Bragg scattering appears as peaks in the scans. In this way it is possible to choose a common "clean" incident neutron energy for all the magnetic reflections considered, indicated by the broken line at  $E_i = 13.4$  meV.

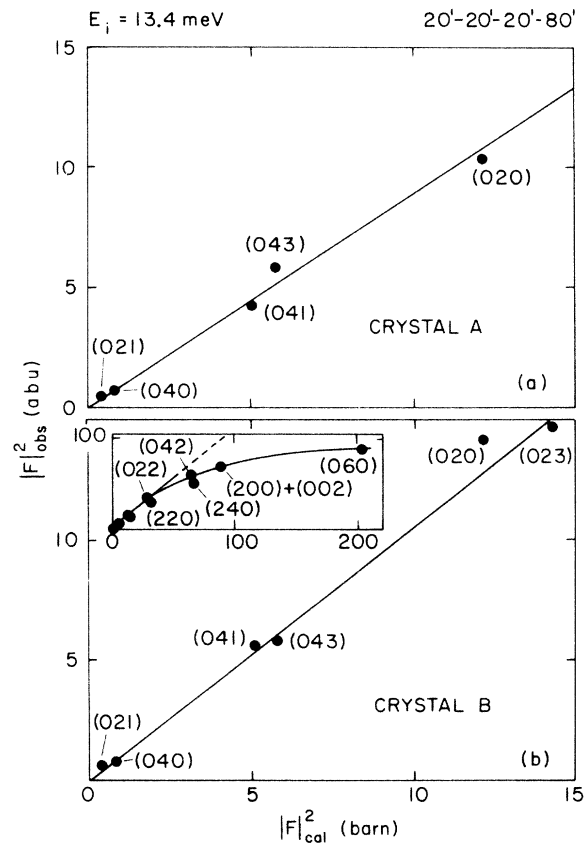


FIG. 3. Plot of the observed  $|F|_{\text{obs}}^2$  vs calculated  $|F|_{\text{cal}}^2$  nuclear structure factors squared for (a)  $\text{La}_2\text{CuO}_4$  crystal A and (b) crystal B. Only the weak reflections ( $|F|^2 < 15$  barn) are shown.  $(0k0)$  intensities are divided by 2 since these peaks arise from the entire crystal while all other reflections only represent one-type twin domain, i.e., approximately half the sample. In the inset, data from the strong reflections are plotted, and the effect of extinction is here seen as a deviation from linearity.

magnetic reflections accessible with the spectrometer at this energy.

In the window around  $E_i = 30.5$  meV it was not possible to achieve a single clean incident energy for the additional magnetic Bragg reflections accessible here. Due to additional interference with aluminum powder lines from the sample container it was only possible to get a clean signal here for the magnetic (500) reflection with the applied crystal orientation. This was obtained at  $E_i = 31.0$  meV.

#### D. Extinction

In order to determine the ordered magnetic moment at low temperature from the intensities of the magnetic reflections, the integrated intensities of nuclear reflections are used for normalization. Therefore, it is very important to measure these correctly and ensure internal consistency between observed and calculated intensities. In order to demonstrate this, all accessible  $(0kl)$  and  $(hk0)$  nuclear intensities were measured for crystal *B* and some of the low-intensity reflections for crystal *A*. The spectrometer was here operated with an incident neutron energy  $E_i = 13.4$  meV, and the observed structure factor  $|F|_{\text{obs}}^2$  was extracted from the raw data by using Eq. (1).

In Fig. 3  $|F|_{\text{obs}}^2$  are plotted versus the calculated values  $|F|_{\text{cal}}^2$ . An arbitrary scale factor was applied to the observed data [matching the (043) reflection]. The linearity between observation and calculations fails to hold for large values of  $|F|^2$ , which indicates that extinction effects are significant for strong reflections, such as (002) or (200). Hence, for normalization purposes only the relatively weak reflections should be used (see Fig. 3). The structure factors  $|F|_{\text{cal}}^2$  were calculated assuming the *Cmca* space group using atomic positions at  $T = 10$  K from powder refinements provided by Jorgensen *et al.*<sup>11</sup>

### III. MAGNETIC SCATTERING

Most of the magnetic reflections accessible for the incident neutron energy  $E_i = 13.4$  meV are shown in Fig. 1. As may be noted from the figure, some of the magnetic and nuclear peaks are very close, e.g.,  $(120)_M$  and  $(021)_N$ . An accurate determination of the integrated intensity in these magnetic peaks is therefore difficult even with the chosen collimation  $20'-20'-20'-80'$ . Hence, for our purpose of determining the magnetic form factor we avoided these peaks and concentrated on  $(100)_M$ ,  $(011)_M$ ,  $(031)_M$ ,  $(051)_M$ ,  $(300)_M$ , and  $(320)_M$ . Using  $E_i = 31.0$  meV the  $(500)_M$  reflection was also measured.

An alternative check of multiple scattering at the magnetic peak positions may be performed by heating the crystal above the antiferromagnetic ordering temperature to be sure that no signal remains. This was done for all the reflections listed above, and all scans appeared clean. Figure 4 shows the  $(100)_M$  reflection at  $T = 10$  K and  $T = 220$  K for illustration.

The  $(100)_M$  peak was used to measure the magnetization curve and determine the Néel temperature for the present crystal. In Fig. 5 the peak intensity of this reflection is shown as a function of temperature and from

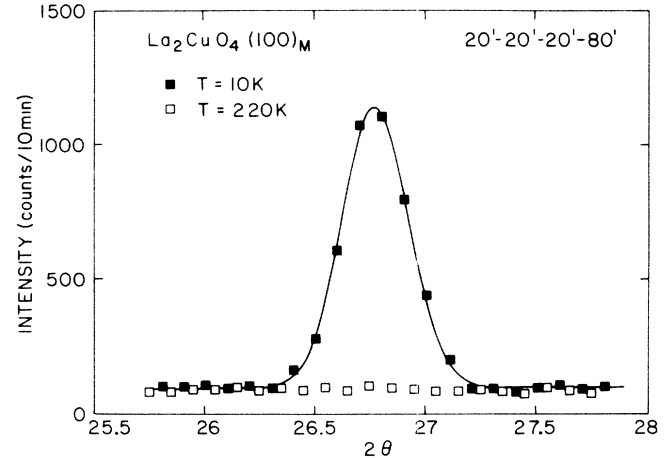


FIG. 4.  $\theta - 2\theta$  scans of the magnetic (100) reflection at  $T = 10$  K and above  $T_N$  at  $T = 220$  K. It is seen that no multiple scattering appears at  $T = 220$  K.

the plot we estimate  $T_N \approx 185$  K. As may be seen, the transition seems to be smeared over the temperature interval from  $\sim 75$  to 185 K. This smearing may be caused by small inhomogeneities in the oxygen deficiency,<sup>5</sup> or other small defects in the crystal. The recent discovery by Shirane *et al.*<sup>12</sup> of a two-dimensional (2D) antiferromagnetic quantum fluid state in  $\text{La}_2\text{CuO}_4$  which is already

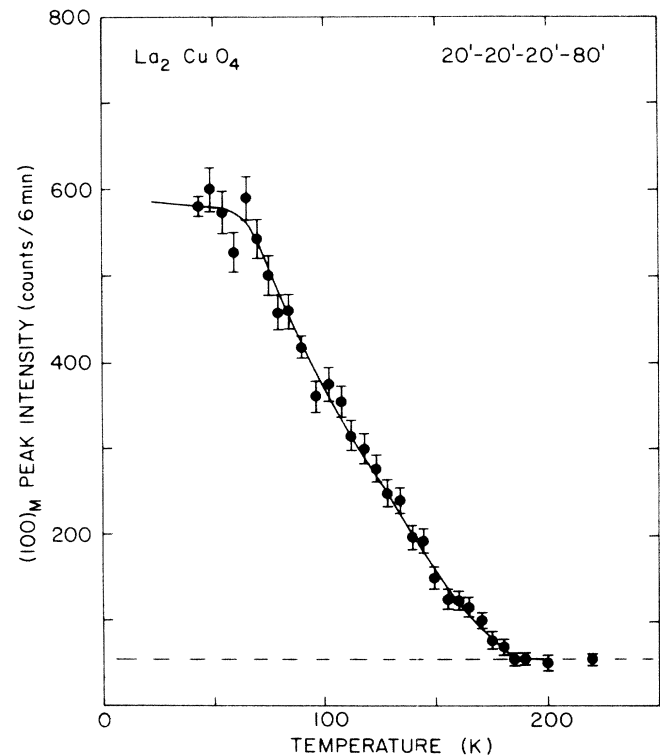


FIG. 5. Peak intensity of the magnetic (100) reflection as a function of temperature. From this plot we estimate the Néel temperature  $T_N = 185$  K. The smearing of the transition is discussed in the text.

present at high temperatures means that the 3D ordering observed at  $T_N$  is merely an ordering of planes. In this case even very small defects in the crystal may play an important role for the 3D ordering, thereby smearing the transition. Note that the mosaic of the crystal is less than  $15'$  (FWHM) measured at the  $(060)_N$  reflection.

We now turn to a discussion of the antiferromagnetic form factor measurements. In Table I is given the integrated background-subtracted intensities for the magnetic and nuclear peaks used in the analysis. Furthermore, for the magnetic reflections  $p$  is given, calculated from Eq. (1) and

$$F = p \langle q \rangle \sum_n \pm \exp[2\pi i(hx_n + ky_n + lz_n)] , \quad (2)$$

where

$$p = \gamma_0 S f(Q)$$

and  $\gamma_0$  is  $0.539 \times 10^{-12}$  cm,  $S$  is the spin,  $f(Q)$  the form factor,  $\langle q \rangle$  the magnetic interaction term, and the sum is over the magnetic atoms in the unit cell. We assume the magnetic structure<sup>3-5</sup> to be described by ferromagnetic sheets of spins altering along the  $[100]$  axis, and the spin direction to be along the  $[001]$  axis. The location of the spins is assumed to be at the Cu atoms which form a face-centered structure. Hence, the scattering from each Cu-atom adds in phase yielding the value 4 for the sum in Eq. (2), independent of  $(hkl)$ . The only  $Q$ -dependent terms in  $F$  are therefore  $\langle q \rangle$  and  $f(Q)$ .

In Fig. 6  $f(Q)$  is plotted as a function of  $Q$  for the reflections measured. The scaling of  $f(Q)$  (i.e., the value of  $S$ ) is slightly arbitrary. We have chosen to scale the data assuming  $f(Q) = 0.835$  for the  $(100)$  reflection.<sup>4,5,7</sup> This value is calculated using a linear interpolation of data from the ferromagnet  $\text{K}_2\text{CuF}_4$  measured by Akimitsu and Ito.<sup>13</sup> In this way the average moment is estimated to  $\mu = gS = 0.30\mu_B$  per Cu atom. Whether this value reflects the true local moment at the Cu site is still in question since muon relaxation measurements<sup>14</sup> on pow-

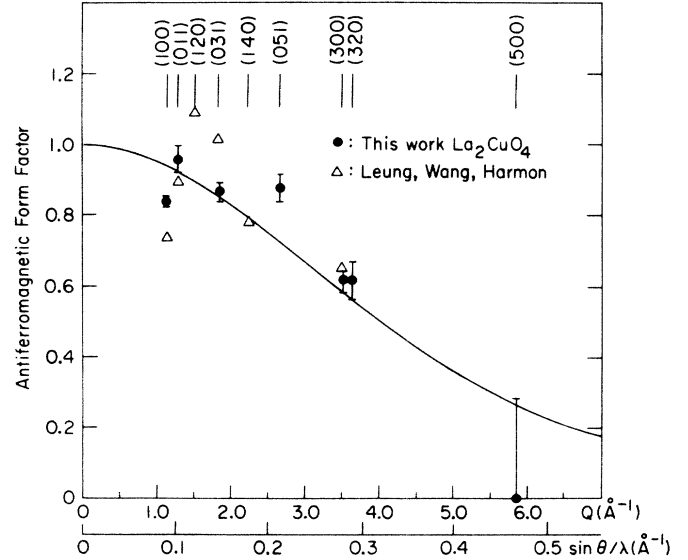


FIG. 6. The antiferromagnetic form factor as a function of  $Q$  or  $\sin\theta/\lambda$ . The solid circles represent the present work with the appropriate magnetic reflection indicated above. To take into account uncertainties in the background, uplining, etc., we have doubled the statistical errors from Table I. The triangles are band-structure calculations for  $\text{Sc}_2\text{CuO}_4$  after Leung, Wang, and Harmon (Ref. 15), and the full curve is the Freeman-Watson  $\text{Cu}^{2+}$  form factor. The calculated values of Ref. 15 have been scaled by 0.77.

der samples of  $\text{La}_2\text{CuO}_4$  indicate that the entire crystal may not be completely ordered.

The solid curve in Fig. 6 is the Freeman and Watson form factor for the free  $\text{Cu}^{2+}$  ion, and recent band-structure calculations by Leung, Wang, and Harmon<sup>15</sup> are also shown. These calculations are made on  $\text{Sc}_2\text{CuO}_4$  using Sc instead of La in order to facilitate the calculations, but the difference is claimed to have only very little effect on the results for the Cu-O interactions. As may

TABLE I. Neutron-diffraction results at  $T = 10$  K for single crystal  $\text{La}_2\text{CuO}_4$ . The numbers in parenthesis are statistical errors on the last digit shown.

$(hkl)$ Magnetic	$Q$ ( $\text{\AA}^{-1}$ )	$\sin\theta/\lambda$ ( $\text{\AA}^{-1}$ )	$\sum I(\theta, 2\theta)$ Counts/ $\sim 10$ min	$ F _{\text{obs}}^2$ ( $10^{-3}$ barn)	$p$ ( $10^{-12}$ cm)	$f(Q)$
(100)	1.17	0.093	3908(70)	66(1)	0.0642(6)	0.835(7)
(011)	1.26	0.100	707(25)	12.7(4)	0.074(1)	0.96(2)
(031)	1.85	0.147	1412(43)	43(1)	0.067(1)	0.87(1)
(051)	2.66	0.211	1091(40)	58(2)	0.067(1)	0.88(2)
(300)	3.52	0.280	488(22)	37(2)	0.048(1)	0.62(1)
(320)	3.64	0.290	478(35)	36(3)	0.047(2)	0.62(2)
(500)	5.87	0.467	0	0	0	0.0(1)
$(hkl)$ Nuclear	$Q$ ( $\text{\AA}^{-1}$ )	$\sin\theta/\lambda$ ( $\text{\AA}^{-1}$ )	$\sum I(\theta, 2\theta)$ Counts	$ F _{\text{obs}}^2$ (arb. units)	$ F _{\text{cal}}^2$ (barn)	
(021)	1.51	0.120	2391	0.47	0.410	
(040)	1.92	0.153	4831/2	0.71	0.828	
(041)	2.24	0.179	5334	4.18	5.06	
(043)	3.98	0.317	3795	5.76	5.76	
(020)	0.96	0.076	79080/2	10.4	12.11	

be seen from the figure, our data are not in very good agreement with the calculated results, although our data are not inconsistent with the free  $\text{Cu}^{2+}$  calculation. The data indicate that the form factor is fairly constant in the  $Q$  interval between 1 and  $3 \text{ \AA}^{-1}$ . This is the same region in which the band-structure calculation<sup>15</sup> exhibits a peak caused by interference between the Cu moment and a small (20%) out-of-plane oxygen contribution. The same effect is found from calculations on this *covalency effect* for  $\text{K}_2\text{CuF}_4$  by Hirakawa and Ikeda.<sup>16</sup> Our results therefore indicate that a very small moment on the out-of-plane oxygen atoms may be present—smaller than 20% suggested by the band-structure calculations. The covalency effect for the in-plane Cu–O bonds does not result in a distribution of moment to these oxygen atoms. Due to the antiferromagnetic order, the contributions here cancel by symmetry. However, the band-structure calculations suggest that each of the in-plane oxygen sites has a fairly large contribution, 55% of the Cu moment, although it may only be observed by inducing a ferromagnetic moment on the sample by an external magnetic field. This point, the distribution of the in-plane spin density, is an issue on which the different theoretical approaches

disagree. At the same time, it may be tested experimentally. Thus, to clarify the problem, the *induced* magnetic form factor can be measured by a neutron-diffraction experiment on  $\text{La}_2\text{CuO}_4$  in a strong magnetic field. Preparations for such an experiment are already in progress.

During the writing of this paper, neutron scattering experiments<sup>12</sup> on a large single crystal of  $\text{La}_2\text{CuO}_4$  have revealed 2D ordering of the spins over long distances already at high temperatures. We note that the rod scattering appearing from this 2D order may be utilized to measure the antiferromagnetic form factor *continuously* as a function of  $Q$  in the out-of-plane direction.

We wish to thank V. J. Emery, Y. Endoh, and Y. J. Uemura for very helpful discussions, and we are grateful to J. D. Jorgensen and B. N. Harmon for sending us details of their results. This work was supported in part by the U.S.–Japan Cooperative Neutron Scattering Program. Work at Brookhaven National Laboratory was supported by the Division of Materials Sciences, U.S. Department of Energy under Contract No. DE-AC02-76CH00016.

<sup>1</sup>J. G. Bednorz and K. A. Müller, *Z. Phys. B* **64**, 189 (1986).

<sup>2</sup>P. W. Anderson, *Science* **235**, 1196 (1987); P. W. Anderson, G. Baskaran, Z. Zou, and T. Hsu, *Phys. Rev. Lett.* **58**, 2790 (1987); V. J. Emery, *ibid.* **58**, 2794 (1987); Y. Hasegawa and H. Fukayama, *Jpn. J. Appl. Phys.* **26**, L322 (1987); J. E. Hirsch, *Phys. Rev. Lett.* **58**, 2691 (1987); S. A. Kivelson, D. S. Rokhsar, and J. P. Sethna, *Phys. Rev. B* **35**, 8865 (1987); P. A. Lee and M. Read, *Phys. Rev. Lett.* **58**, 2691 (1987).

<sup>3</sup>D. Vaknin, S. K. Sinha, D. E. Moncton, D. C. Johnston, J. Newsam, C. R. Safinya, and H. King, *Phys. Rev. Lett.* **58**, 2802 (1987).

<sup>4</sup>S. Mitsuda, G. Shirane, S. K. Sinha, D. C. Johnston, M. Alvarez, D. E. Moncton, and D. Vaknin, *Phys. Rev. B* **36**, 822 (1987); B. X. Yang, S. Mitsuda, G. Shirane, Y. Yamaguchi, H. Yamauchi, and Y. Syono, *J. Phys. Soc. Jpn.* **56**, 2283 (1987).

<sup>5</sup>T. Freltoft, J. E. Fischer, G. Shirane, D. E. Moncton, S. K. Sinha, D. Vaknin, J. P. Remeika, A. S. Cooper, and D. Harshman, *Phys. Rev. B* **36**, 826 (1987).

<sup>6</sup>D. C. Johnston, J. P. Stokes, D. P. Goshorn, and J. T. Levanowski, *Phys. Rev. B* **36**, 4007 (1987).

<sup>7</sup>K. Yamada, E. Kudo, Y. Endoh, Y. Hidaka, M. Oda, M. Suzuki, and T. Murakami (unpublished).

<sup>8</sup>V. B. Grande, H. Müller-Buschbaum, and M. Schwazer, *Z. Anorg. Allg. Chem.* **428**, 120 (1979).

<sup>9</sup>M. Onoda, S. Shamoto, M. Sato, and S. Hosoya, *Jpn. J. Appl. Phys.* **26**, L363 (1987); Y. Hirotsu, S. Nagakura, Y. Murata, T. Nishihara, M. Takata, and T. Yamashita, *ibid.* **26**, L380 (1987).

<sup>10</sup>C. H. Chen (private communication).

<sup>11</sup>J. D. Jorgensen, H.-B. Schüttler, D. G. Hinks, D. W. Capone II, K. Zhang, and M. B. Brodski, *Phys. Rev. Lett.* **58**, 1024 (1987); J. D. Jorgensen (private communication).

<sup>12</sup>G. Shirane, Y. Endoh, R. J. Birgeneau, M. A. Kastner, Y. Hidaka, M. Oda, M. Suzuki, and T. Murakami, *Phys. Rev. Lett.* **59**, 1613 (1987).

<sup>13</sup>J. Akimitsu and Y. Ito, *J. Phys. Soc. Jpn.* **40**, 1621 (1976).

<sup>14</sup>Y. J. Uemura, W. J. Kossler, X. H. Yu, J. R. Kempton, H. E. Schone, D. Opie, C. E. Stronach, D. C. Johnston, M. S. Alvarez, and D. P. Goshorn, *Phys. Rev. Lett.* **59**, 1045 (1987).

<sup>15</sup>T. C. Leung, X. W. Wang, and B. N. Harmon, *Phys. Rev. B* **37**, 384 (1988).

<sup>16</sup>K. Hirakawa and H. Ikeda, *Phys. Rev. Lett.* **33**, 374 (1974).